15.4   SIMULTANEOUS HORIZONTAL AND VERTICAL TRANSMIT RADAR DATA AND POLARIZATION ERRORS

J.C. Hubbert,[*] M. Dixon, S. Ellis and G. Meymaris

National Center for Atmospheric Research, Boulder CO

1. INTRODUCTION

The simultaneous transmission and reception of H (horizontal) and V (vertical) polarized waves (called SHV mode) has become a very popular way to achieve dual polarization for weather radar (Doviak et al. 2000). The advantage is that a fast polarization switch is not necessay to achieve dual polarization data. The disadvantages are 1) that the linear depolarization ratio (LDR) is not measured and 2) that there can be cross-coupling of the H and V waves which will lead to biases in the measurement of of H and V reflectivities Z_H and Z_V, and the crosscorrelation coefficient $\rho_{hv} = |\rho_{hv}| \exp\{\Psi_{dp}\}$ where $\Psi_{dp} = \phi_{dp} + \delta$. ϕ_{dp} is the differential propagation phase while δ is the differential backscatter phase. The viability of this dual polarization technique is base on 1) non-zero mean canting angle of the propagation medium, and 2) negligible antenna polarization errors. If either condition is not met, cross-coupling between the H and V channels occurs which will cause measurement biases.

Measurement errors in the SHV mode have been investigated. Doviak et al. (2000) evaluated cross-coupling errors of SHV mode and concluded that since the mean canting angle of rain is zero, the errors were acceptable. Wang and Chandrasekar (2006) investigated the measurement errors in Z_H, Z_{dr}, Ψ_{hv} and ρ_{hv} due to cross-coiupling errors caused by the radar system as a function of ϕ_{dp}. They concluded that system isolation between the the H and V channels must be greater than -44 dB in order to insure the Z_{dr} bias is with 0.2 dB for worst case errors.

Ryzhkov and Zrnić (2007) examined the effects of non-zero mean canting angle of the precipitation medium on SHV mode measurements. Data gathered in SHV mode with KOUN displayed Z_{dr} radial bias "stripes" after the radar waves passed through the ice phase of either convective cells or stratiform precipitation. They propose that non-zero mean canting angle of the propagation medium causes coupling between the H and V polarized waves that causes the anomalous Z_{dr} signatures.

In this paper, cross-coupling due to non-zero mean canting angle and antenna errors are investigated, first via a radar data model and second with experimental data.

---

[*]NCAR/EOL, Boulder, Colorado 80307, email: hubbert@ucar.edu

Transmit errors are also included separately in the model by specifying the transmit polarization state that is fed to the antenna.

All reflector type antennas will introduce some distortion to the desired H and V transmit polarization states causing cross coupling between the H and V polarization states. This will bias polarization measurements of precipitation. These errors are analogous to the cross-coupling problem reported in Ryzhkov and Zrnić (2007). This paper investigates the impact of antenna induce cross-coupling errors caused by the non ideal radar antenna. The radar model introduced by Hubbert and Bringi (2003) is used to quantify the impact of polarization errors on Z_{dr} and ϕ_{dp}. Finally experimental data from S-Pol, NCAR's S-band polarimetric radar, are used to illustrate the theory. Recently, S-Pol collected data in fast alternating H and V mode (referred to as FHV mode) quickly followed by data collected in simultaneous H and V transmit mode (referred to as SHV mode). These data clearly illustrate the effects of antenna polarization errors. This is the first time that such data has been collected.

2. MODELING POLARIZATION ERRORS AND CROSS-COUPLING

The scattering model used is described in Hubbert and Bringi (2003) but is briefly reviewed here. The particles in the backscatter volume and the coherent propagation medium are independently modeled. The "steady" propagation medium is modeled via a 2×2 matrix that includes absolute attenuation (A_h), differential attenuation (A_{dp}), differential propagation phase (ϕ_{dp}) and mean canting angle (θ) as parameters. The resolution volume (or backscatter medium) is modeled as an ensemble of precipitation particles with Gamma DSD (drop size distribution) and arbitrary spatial orientation distributions via the T-matrix method (Vivekanandan et al., 1991; Waterman, 1969). The modeled parameters can be independently varied so that the sensitivity of the crosspolar and co-to-cross covariances can be studied. Antenna polarization errors are modeled similar to McCormick (1981).

The scattering geometry used is the BSA (backscatter alignment) convention (Bringi and Chandrasekar 2001) Canting angles are measured counterclockwise from the

horizontal in the plane of polarization (i.e., plane containing H and V axes perpendicular to the propagation direction).

Since forward scatter is coherent (van de Hulst, 1957), the propagation medium can be completely described via a 2×2 scattering matrix, $\mathbf{P}$, as

$$\mathbf{P} = \mathbf{R}(-\theta)\mathbf{P_0}\mathbf{R}(\theta) \tag{1}$$

where $\mathbf{R}$ is the Cartesian rotation matrix and $\mathbf{P_0}$ is the principal plane propagation matrix

$$\mathbf{P_0} = \left[\begin{array}{cc} e^{\{\lambda_1 z\}} & 0 \\ 0 & e^{\{\lambda_2 z\}} \end{array} \right] \tag{2}$$

where $\lambda_{1,2}$ are the complex propagation constants along the principal planes of the propagation medium and z is the distance along the direction of propagation

In this paper, the antenna polarization errors and cross coupling caused by non-zero mean canting angle are the focus and the backscatter medium is not considered. The mean tilt angle, α, and mean ellipticity angle , ϵ are of the backscatter medium set to zero and this implies that the co-to-cross covariance terms in the backscatter 3×3 covariance matrix are zero. The general form of the propagation-modified covariance matix is (Tragl 1990)

$$\mathbf{\Sigma}_0 = \left[\begin{array}{ccc} \langle |S_{aa}|^2 \rangle & \sqrt{2}\langle S_{aa}S_{ab}^* \rangle & \langle S_{aa}S_{bb}^* \rangle \\ \sqrt{2}\langle S_{ab}S_{aa}^* \rangle & 2\langle |S_{ab}|^2 \rangle & \sqrt{2}\langle S_{ab}S_{bb}^* \rangle \\ \langle S_{bb}S_{aa}^* \rangle & \sqrt{2}\langle S_{bb}S_{ab}^* \rangle & \langle |S_{bb}|^2 \rangle \end{array} \right] \tag{3}$$

where $\langle * \rangle$ denote ensemble average.

2.1 *Antenna polarization errors*

The radar antenna and surrounding microwave circuitry introduce microwave cross-coupling that give rise to polarization errors so that pure H or V polarization are not transmitted. Polarization errors have been covered in detail by McCormick (1981). Some of the sources of polarization error are non-ideal feed horn, non ideal parabolic reflector, antenna support struts and edge effects. These polarization errors are distributed across the radar antenna patterns and thus can vary across the beam especially where the cross-polarized lobes exist (Bringi and Chandrasekar 2001). For distributed precipitation media, the resulting error is an integrated effect and we model these distributed errors with a 2×2 polarization error matrix.

The polarization errors are easily included in the model by pre- and post- multiplying $\mathbf{S}$, the 2×2 backscatter matix, by the error matrix $\mathbf{\Upsilon}$

$$\mathbf{S_e} = \mathbf{\Upsilon}^T \mathbf{S} \mathbf{\Upsilon} \tag{4}$$

where

$$\mathbf{\Upsilon} = \left[\begin{array}{cc} i_h & \varepsilon_v \\ \varepsilon_h & i_v \end{array} \right] . \tag{5}$$

with constraints $i_h^2 + |\varepsilon_h|^2 = i_v^2 + |\varepsilon_v|^2 = 1$ with i_h, i_v real. The polarization errors of the H and V channels are represented by the complex numbers ε_h and ε_v, respectively. The polarization errors can also be equivalently represented with the geometric ellipse parameters of tilt angle, τ and ellipticity angle, ϵ. These variables are related by (Azzam and Bashara, 1989)

$$\tan 2\tau = \frac{2\Re(\chi)}{1 - |\chi|^2} \tag{6}$$

$$\sin 2\epsilon = \frac{2\Im(\chi)}{1 + |\chi|^2} \tag{7}$$

where χ is the polarization ratio define by $\chi = E_v/E_h$ where E_v and E_h are the vertical and horizon electric field components, and $\Re$ and $\Im$ denote real and imaginary parts, respectively. For H errors, $\chi = \varepsilon_h/i_h$ and for V errors, $\chi = i_v/\varepsilon_v$. As can be seen from the equations, if the ε_h (ε_v) is real then ϵ is zero and if ε_h (ε_v) is imaginary then τ is zero. If the errors are orthogonal, i.e., $\varepsilon_v = -\varepsilon_h^*$, then $\mathbf{\Upsilon}$ is unitary and (4) represents an orthogonal change of polarization basis. Separating the polarization errors into their geometric components gives a convenient and intuitive way to analyze polarization errors.

2.2 *Modeling Simultaneous H and V transmissions*

These model thus far was constructed under the assumption that the radar is operating in FHV (fast alternating H and V) mode. The covariance matrix of Eq.(3) is a convenient form for to express the radar covariances and for polarization bases transformations; however, it does not function as a transmission matrix, i.e., it does not express a transfer relationship between an arbitrary input polarization and the resultant output covariances such as the 4×4 Mueller matrix does (Bringi and Chandrasekar 2001). In order to model output covariances that result from arbitrary transmit polarizations, a 4×4 covariance matrix is formed using the feature vector

$$\mathbf{\Omega}^T = [S_{HH}\ S_{VH}\ S_{HV}\ S_{VV}] \tag{8}$$

Taking the outer product of of the feature vector gives the covariance matrix in the H-V basis as

$$\mathbf{\Sigma}_0 = \left[\begin{array}{cc} \langle |S_{HH}|^2 \rangle & \langle S_{HH}S_{VH}^* \rangle \\ \langle S_{VH}S_{HH}^* \rangle & \langle |S_{VH}|^2 \rangle \\ \langle S_{HV}S_{HH}^* \rangle & \langle S_{HV}S_{VH}^* \rangle \\ \langle S_{VV}S_{HH}^* \rangle & \langle S_{VV}S_{VH}^* \rangle \end{array} \right.$$

$$\begin{array}{cc} \langle S_{HH}S_{HV}^*\rangle & \langle S_{HH}S_{VV}^*\rangle \\ \langle S_{VH}S_{HV}^*\rangle & \langle S_{VH}S_{VV}^*\rangle \\ \langle |S_{HV}|^2\rangle & \langle S_{HV}S_{VV}^*\rangle \\ \langle S_{VV}S_{HV}^*\rangle & \langle |S_{VV}|^2\rangle \end{array} \Bigg] \qquad (9)$$

where $\langle\cdot\rangle$ denotes spatial or temporal averages. Note that the covariance matrix is Hermitian. It an be shown that the matrix of Eq.(9) is easily transformed to the Mueller matrix and thus the covariance matrix of Eq.(9) can also be used as a transfer function matrix

$$\mathbf{J_o} = \mathbf{\Sigma}_0\,\mathbf{J}_i \qquad (10)$$

where $\mathbf{J}_i$ and $\mathbf{J}_o$ are 1×4 input and output coherency matrices. In terms of the desired polarization characteristics of the incident polarization, namely tilt angle (α) and ellipticity angle (ϵ), $\mathbf{J}_i$ becomes

$$\mathbf{J}_i = \begin{bmatrix} J_{i1} \\ J_{i2} \\ J_{i3} \\ J_{i4} \end{bmatrix} = \begin{bmatrix} 1 + \cos 2\alpha \cos 2\epsilon \\ \sin 2\alpha \cos 2\epsilon - j\sin 2\epsilon \\ \sin 2\alpha \cos 2\epsilon + j\sin 2\epsilon \\ 1 - \cos 2\alpha \cos 2\epsilon \end{bmatrix} \qquad (11)$$

If linear slant $45°$ incident is desired (i.e. SHV mode), then $\alpha = 45°$ and $\epsilon = 0°$. The SHV variables of interest can be calculated as

$$Z_{dr}^{hy} = 10\log_{10}[J_{o1}/J_{o4}] \qquad (12)$$

$$\Psi_{dp}^{hy} = \tan^{-1}(\Im\{J_{o3}\}/\Re\{J_{o3}\}) \qquad (13)$$

$$\rho_{hv}^{hy} = \frac{|J_{o2}|}{\sqrt{|J_{o1}||J_{o4}|}} \qquad (14)$$

where the superscript denotes hybrid mode or SHV mode.

3. MODEL RESULTS

Next we examine biases in Z_{dr}^{hy} caused by 1) transmit errors, and 2) non-zero mean propagation canting angle. Antenna polarization errors. are considered later. Again, the radar variables are plotted as a function of principle plane ϕ_{dp}^P. Since ϕ_{dp}^P is the independent variable and since K_{dp} i is of more meteorological interest than ϕ_{dp}, normalize hybrid K_{dp} is expressed as:

$$K_{dp}^{Nhy} = \frac{K_{dp}^{hy}}{K_{dp}^P} \qquad (15)$$

where K_{dp}^{Nhy} is normalize hybrid K_{dp}, K_{dp}^{hy} is hybrid K_{dp} and K_{dp}^P is principle plane K_{dp}. Absolute attenuation $A_h = 0.0165$ dB/deg. and differential attenuation $A_{dp} = 0.0035$ dB/deg. which are typical S-band values.

3.1 *Transmit Errors*

Z_{dr}^{hy} is plotted as a function of ϕ_{dp}^P. The transmit polarization state is specified with the complex transmit H and V electric fields, E_h^t and E_v^t. This is not the electric field that emerges from the the antenna but is rather the electric field that in injected into the wave guides that feed the antenna. For SHV mode, ideally $E_h^t = E_v^t$. Figure 1 shows Z_{dr} when $|E_h^t| \neq |E_v^t|$, the mean canting angle of the precipitation medium is zero degrees and the antenna polarization are zero, i.e., $\varepsilon_h = \varepsilon_v = 0$. The Z_{dr} bias is independent of the phase difference between E_h^t and E_v^t. The slope of the curves is caused by $A_{dp} = 0.0035$dB/deg. The red nominal line is considered ideal. As can be seen the biases are constant as compared to the nominal curve and such biases could be corrected via calibration.

3.2 *Non-zero mean canting angle*

The model is now used to illustrate Z_{dr} bias caused by non-zero mean canting angle of the propagation medium. Antenna errors are zero and the transmit errors are zero, i.e., $E_h^t = E_v^t$. Figure 2 shows just the Z_{dr} bias as a function of ϕ_{dp}^P with the mean canting angle of the propagation medium as a parameter. As the mean canting angle increases, the bias increases. If the pricipal plane $\phi_{dp} < 10°$, the biases are kept to within about 0.1 dB. Figure 3 is similar to Fig. 2 except that the phase difference between E_h^t and E_v^t is $90°$, i.e., the transmit polarization is circular. The Z_{dr} bias (the difference between the SHV mode Z_{dr} and the nominal line) now increases much more rapidly as a function of ϕ_{dp}^P as compared to Fig. 2. Now ϕ_{dp}^P needs to be less than about 1 degree in order to kept Z_{dr} bias less than about 0.1 dB. This then shows that if the mean canting angle of ice particles is not zero, very little differential phase needs to accumulate in order to cause significant Z_{dr} bias. This corroborates the research of Ryzhkov and Zrnić (2007).

4. ESTIMATING ANTENNA POLARIZATION ERRORS

The estimation of the complex error terms, ε_h and ε_v, is difficult and they are typically not supplied by the manufacturer. There are ways, however, to estimate the magnitude of the error terms and to generally qualify their character. Two available quantities are, LDR (Linear Depolarization Ratio) and passive sun calibration measurements.

LDR can be expressed as a function of the polarization errors ε_h and ε_v (Bringi and Chandrasekar 2001). The radar system lower limit of LDR can be estimated by measurements in drizzle where raindrops are considered circular so that the intrinsic LDR is $-$ inf dB. Measured LDR is then an estimate of the radar system iolation be-
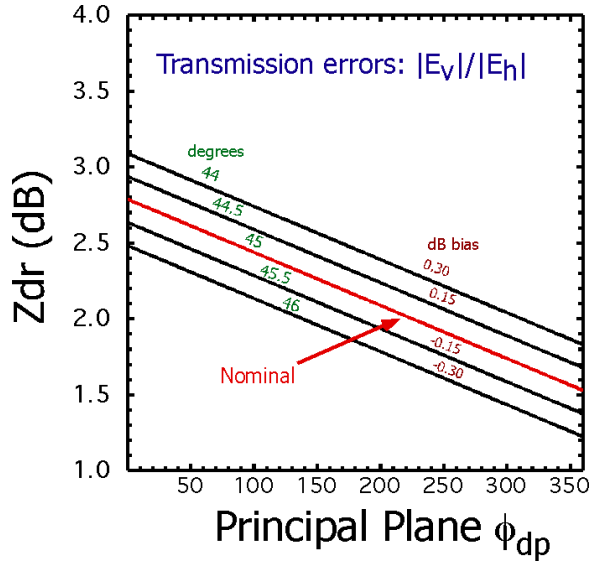
Figure 1: Z_{dr} as a function of principal plane ϕ_{dp} with unbalanced transmit power as a parameter. For SHV mode, $|E_h^t| = |E_v^t|$ and this curve is shown as nominal in red. The errors are independent of the phase difference between E_h^t and E_v^t.
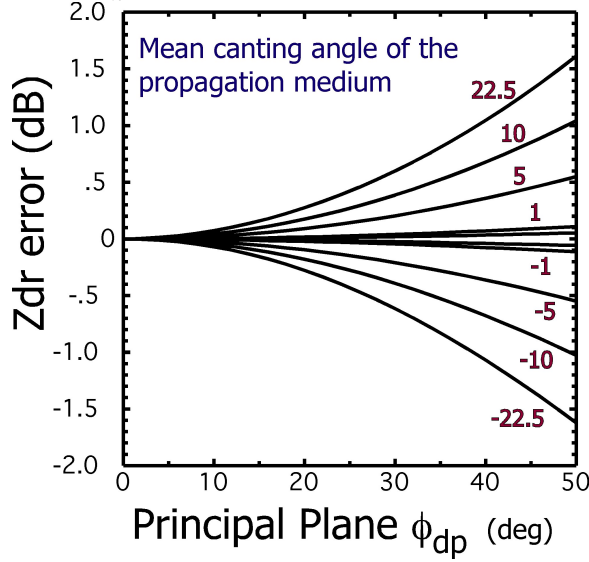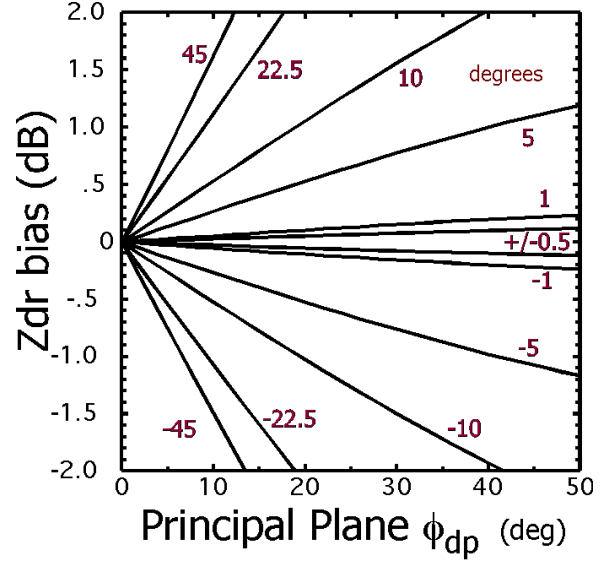

Figure 2: Z_{dr} bias as a function of principal plane ϕ_{dp} with the mean canting angle of the propagation medium as a parameter. There transmission errors are zero, i.e., $|E_h^t| = |E_v^t|$. The errors are independent of the phase difference between E_h^t and E_v^t.

Figure 3: Z_{dr} bias as a function of principal plane ϕ_{dp} with the mean canting angle of the propagation medium as a parameter. $|E_h^t| = |E_v^t|$ but there is a 90° phase difference, i.e., circular polarization is transmitted.

tween the H and V channels. For well designed radars, the dominant cross coupling factor is the antenna. The received electric-fields can be modeled in drizzle as

$$
\begin{bmatrix} E_h^r \\ E_v^r \end{bmatrix} = \begin{bmatrix} i_h & \varepsilon_h \\ \varepsilon_h & i_v \end{bmatrix} \begin{bmatrix} 1 & 0 \\ 0 & 1 \end{bmatrix} \begin{bmatrix} i_h & \varepsilon_v \\ \varepsilon_h & i_v \end{bmatrix} \begin{bmatrix} E_h^i \\ E_v^i \end{bmatrix} \quad (16)
$$

where the identity matrix is the backscatter matrix for drizzle. For transmit state $E_h^i = 1$, $E_v^i = 0$, LDR is

$$
LDR = \frac{|\langle \varepsilon_v i_h + \varepsilon_h i_v \rangle|^2}{|\langle i_h^2 + \varepsilon_h^2 \rangle|^2} \quad (17)
$$

Using the approximations $|\varepsilon_{h,v}| \ll i_{h,v}$ and $i_h = i_v \approx 1$, it follows that

$$
LDR = |\varepsilon_h + \varepsilon_v|^2 = |\varepsilon_h|^2 + |\varepsilon_v|^2 + 2\Re\{\varepsilon_v \varepsilon_h^*\} \quad (18)
$$

where $\Re$ stands for the the real part.

The LDR system limit values are typically in the -30 to -34 dB range for well designed radars. If $\varepsilon_h = \varepsilon_v$ and ε_h and ε_v are real (or imaginary) then $LDR = 10\log_{10}(2\varepsilon_h)^2 = -30$ dB, and therefore $\varepsilon_h = \varepsilon_v = 0.0158$. If the the LDR limit is -35 dB, then $\varepsilon_h = \varepsilon_v = 0.00889$. Equivalently, these errors correspond to a tilt and ellipticity angles of the polarization state (polarization ellipse) of the received wave. The angles are 0.91○ and 0.51° for LDR limits of -30 dB and -35 dB, respectively. If the ε_h and ε_v are real, the angles are tilt angles, and if the ε_h and ε_v are imaginary, the angles are ellipticity angles.

4.1 *Solar scan measurements*

The solar data is collected performing a "box scan" of the the sun in passive mode. The sun here is considered as an unpolarized RF source that has a width of about 0.53° (Tapping 2001). The dimension of the box scan is approximately 5° high (elevation angle) by 8° wide (in azimuth). Noise samples are collected while the radar is pointing away from the the sun so that the thermal background noise can be estimated and used to correct the measured sun data. The typical scanning rate is $1°\text{s}^{-1}$. The data is interpolated to a square 2° by 2° in 0.1° intervals. The data is first corrected for sun movement and distortion caused by scanning in elevation and azimuth angle rather than in a rectangular grid. Shown in Fig. 4 are the H and V pseudo antenna patterns obtained from such solar scans. These are termed pseudo antenna patterns since the sun is not a point source and thus the given antenna patterns are a convolution of the antenna beam pattern of S-pol with the 0.53° solar disk. The complex H and V antenna data can be used to create a correlation antenna pattern. The receive voltage time series, $E_h^r(i)$ and $E_v^r(i)$ for the H and V patterns, respectively, are correlated in typical fashion as

$$\omega = \frac{\sum_{i=1}^{N} E_h(i)E_v^*(i)}{\sqrt{\sum_{i=1}^{N} E_h(i)E_h^*(i) \sum_{i=1}^{N} E_v(i)E_v^*(i)}} \quad (19)$$

This data can also be interpolated to a grid. The resulting magnitude and phase of the correlation product of Eq.(19) are give in Fig. 5. Since the sun radiation is unpolarized, the correlation between any two orthogonal polarization state should be zero. The top panel of the figure shows two principal "lobes" in the lower two quadrants where the correlation increases to about 0.07. These large areas of increased correlation coefficient are manifestation of the antenna polarization errors. The cross-correlation is obviously a function of azimuth and elevation angle and is not constant across the 2° by 2° antenna patterns shown. The areas of maximum correlation do, however, fall outside the 3 dB beamwidth of the antenna which is about 1°. The bottom panel of Fig. 5 shows the complex behavior of the phase of the correlation products with the phases being fairly constant in the regions of highest correlation. For the lower left quadrant this phase is -100° while the lower right quadrant phase is about 60°.

The radar model presented above represents the antenna polarization errors as a single complex number numbers for the H and V polarization, i.e., the polarization errors are considered constant across the entire radar antenna pattern. Even though this is not true, it is a useful approximation that simplifies analysis and permits a "first order" evaluation and simulation of polarization errors.
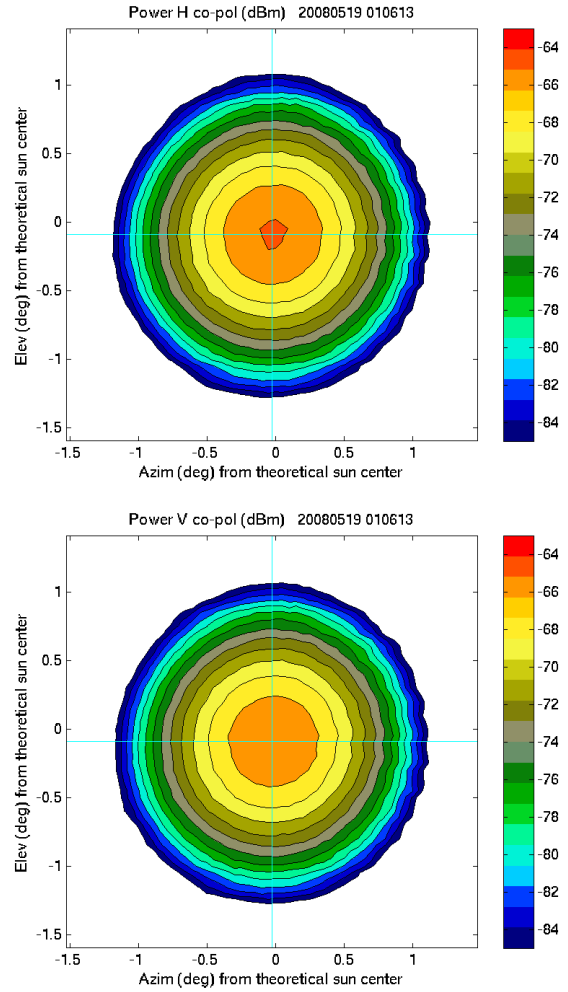

Figure 4: *Pseudo H (top) and V (bottom) S-Pol antenna patterns obtained by scanning the sun passively.*
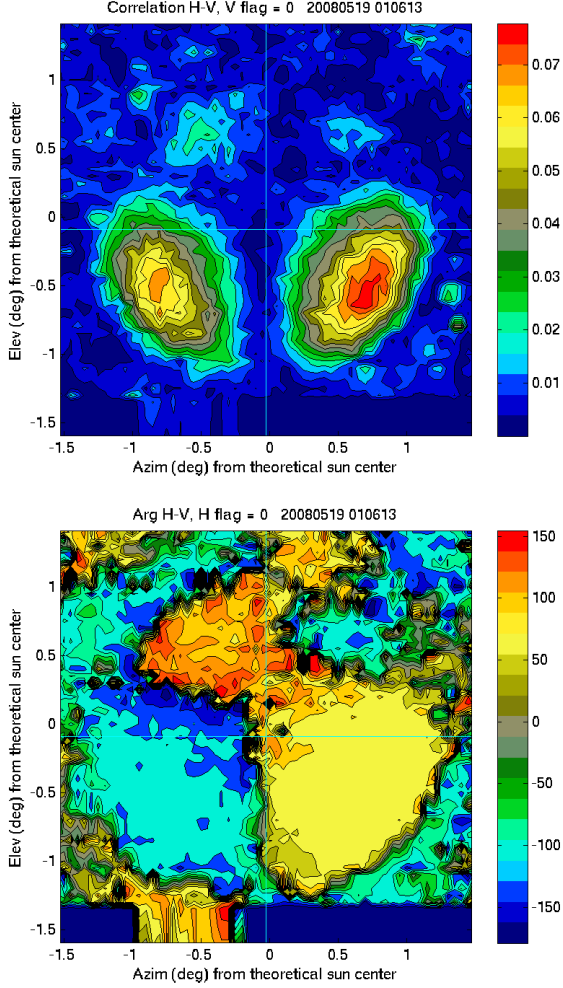
Figure 5: *Pseudo H to V correlation S-Pol antenna patterns obtained by scanning the sun passively. Top panel in the magnitude and the bottom panel is differential phase.*

It can be shown that for small polarization errors, ε_h and ε_v,

$$\Omega = \varepsilon_h^* + \varepsilon_v \tag{20}$$

where Ω is the pattern integrated correlation coefficient and ε_h and ε_v are the antenna polarization errors as given in Eq.(5). Thus, the correlation products are averaged across the entire given 2° by 2° correlation beam pattern of Fig. 5 to arrive at a single complex number. This would be valid if the radar is scanning a uniform, homogeneous region.

Solving Eqs.(18) and (20) simultaneously yields

$$\Im\{\varepsilon_v\} = \frac{\Im\{\Omega\} \pm \sqrt{\Im^2\{\Omega\} - 4(|\Omega|^2 - LDR)}}{2} \tag{21}$$

$$\Im\{\varepsilon_h\} = \frac{-\Im\{\Omega\} \mp \sqrt{\Im^2\{\Omega\} - 4(|\Omega|^2 - LDR)}}{2} \tag{22}$$

In term of the voltages, the solutions are

$$\Im\{\varepsilon_h\} = \frac{\Im\{ldr\} - \Im\{\Omega\}}{2} \tag{23}$$

$$\Im\{\varepsilon_v\} = \frac{\Im\{ldr\} + \Im\{\Omega\}}{2} \tag{24}$$

The real parts are not solvable but it can be shown they obey the condition

$$\Re\{ldr\} - \Re\{\Omega\} = 0 \tag{25}$$

where ldr is the complex number $\varepsilon_h + \varepsilon_v$ (see Eq.(18)).

4.2 *Antenna errors*

Figure 6 show SHV mode Z_{dr} for one degree polarization tilt errors (upper panel) and one degree polarization ellipticity errors (lower panel). Such errors correspond to an LDR system limit of about -30 dB. The solid straight lines represent non-baised Z_{dr} that would be measured in fast alternating transmit mode. As can be seen, Z_{dr} errors are significant with a maximum error of about 0.6 dB.

Figure 7 shows Z_{dr} bias for mixed tilt and ellipticity angles. The H and V tilt and ellipticity angles are given in Table 1. As can be seen, the character of the Z_{dr} bias is quite different for each curve with the maximum bias is about 0.4 dB for each curve. This antenna errors all correspond to about a -31 dB system LDR limit.

5. EXPERIMENTAL SHV DATA

During May and June 2008, S-Pol was deployed in Southern Taiwan for the field experiment TiMREX (Terrain-influenced Monsoon Rainfall Experiment) where data were collected in the SHV mode. Normally
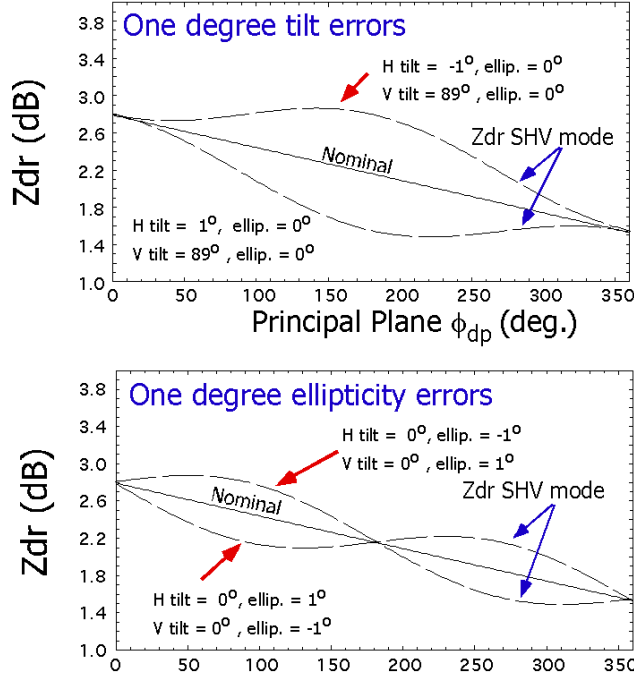
Figure 6: *SHV mode Z_{dr} for one degree antenna polarization errors. The upper panel shows $\pm 1°$ tilt errors while the lower panel shows $\pm 1°$ ellipticity errors.*
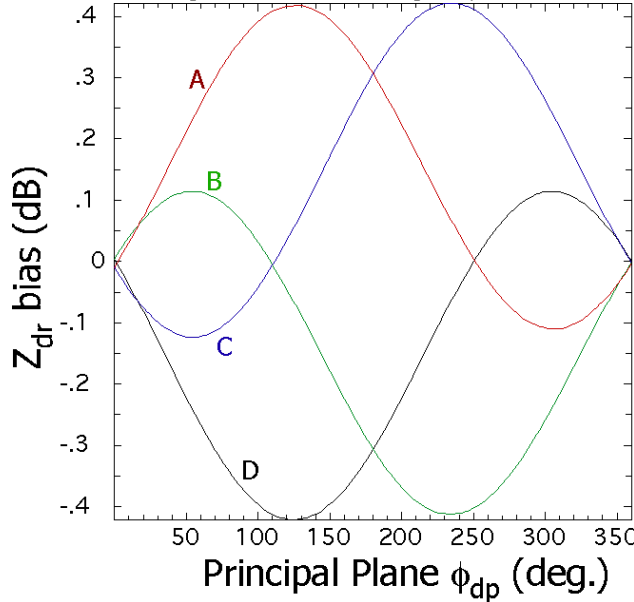

Figure 7: *SHV mode Z_{dr} for mixed tilt and ellipticity antenna error angles which are given in Table 1. These antenna error corespond to a system LDR limit 0s -30 dB.*

	H tilt	H ellip.	V tilt	V ellip.
A	-0.5°	-0.7°	89.5°	0.7°
B	0.5°	-0.7°	90.5°	0.7°
C	-0.5°	0.7°	89.5°	-0.7°
D	0.5°	0.7°	90.5°	-0.7°

Table 1: *The H and V tilt and ellipticity error angles corresponding to 7.*

S-Pol operates in the FHV mode. Thus, SHV and FHV data that were gathered only minutes apart can be compared. Two cases are examined: 1) 8.6° elevation data and 2) 2.0° elevation data. The first case demonstrates Zdr bias due to non-zero mean canting angle and the second data set demonstrates Z_{dr} bias due to antenna polarization errors.

5.1 *8.6° elevation data*

Figures 8 and 9 show S-Pol FHV mode reflectivity (Z) and differential reflectivity (Z_{dr}) gathered during TiMREX on 2 June 2008, 6:19:36 UTC at 8.6° elev. Figures 10 and 11 show SHV Z and Z_{dr} gathered at 6:13:59 UTC at 8.6° elev. A line of convective cells is on the eastern edge with trailing stratiform rain to the west. Storm cells were moving west to east. At about 35 km range, high and noisy Z_{dr} marks the brightband. Note the azimuthal "striping" of Z_{dr} in the SHV mode Z_{dr} data beyond the brightband in Fig. 11. No Z_{dr} striping is evident in the FHV Z_{dr} data of Fig. 8. The Z_{dr} striping in Fig. 11 is likely due to non-zero mean canting angle of the ice particles in the propagation path in agreement with the results presented by Ryzhkov and Zrnić (2007).

5.2 *2.0° elevation data*

Figures 12 and 13 show S-Pol FHV mode reflectivity (Z) and differential reflectivity (Z_{dr}) gathered during TiMREX on 2 June 2008, 6:17:06 UTC at 2.0° elev. Figures 14 and 15 show SHV Z and Z_{dr} gathered at 6:11:28 UTC at 2.0° elev. There is no Z_{dr} striping evident in the SHV data of Fig. 15 since the elevation angle is low and most of the data is in rain which has zero mean canting angle. The SHV and FHV Z_{dr} data appear fairly comparable but in fact there is a bias in the SHV data. To show this, we employ the self consistency Z calibration technique of Vivekanandan et al. (2003). The technique is based on the relationship of Z, Z_{dr} and ϕ_{dp} in rain. Based on the typical range of rain drop size and shape distributions, ϕ_{dp} can be estimated based on measured Z and Z_{dr}. This estimated ϕ_{dp} (ϕ_{dp}^e) is compared to the measured ϕ_{dp} (ϕ_{dp}^m). A scatter plot is generated and a

straight line fit is calculated. If the calculated mean line differs from the 1-to-1 line, this indicates a reflectivity bias. The technique assumes that Z_{dr} is well calibrated (S-Pol Z_{dr} is calibrated via vertical pointing data in light rain).

Shown in Fig.16 is a scatter plot of ϕ_{dp}^e versus ϕ_{dp}^m for TiMREX data. The Z bias is about 0.03 dBZ, i.e., negligible. Note the tight scatter about the 1-to-1 line. This indicates that that S-Pol is well calibrated and such self consistency plots are the norm for S-Pol. Fig. 17 is similar to Fig. 16 except the data was gathered in FHV mode. The scatter is rather tight about the 1-to-1 line for $\phi_{dp} < 50°$ but for $\phi_{dp} > 70°$ the computed ϕ_{dp} are biased low. We believe that this is due to biased SHV Z_{dr}.

To further illustrate this SHV Z_{dr} bias, Z_{dr} is averaged under the constraint $20\,\text{dBZ} < Z, 25\,\text{dBZ}$. These Z_{dr} data are partitioned into three categories: 1) $20° < \phi_{dp} < 40°$, 2) $40° < \phi_{dp} < 70°$, and 3) $70° < \phi_{dp} < 100°$. The results are given in Table 2. For low ϕ_{dp} the SHV and FHZ Z_{dr} values are about equal. For $40° < \phi_{dp} < 70°$, the Z_{dr}s differ by 0.11 dB and for $70° < \phi_{dp} < 100°$ the Z_{dr}s differ by 0.27 dB. The data is not corrected for differential attenuation. This increasing difference between FHV and SHV Z_{dr} as a function of ϕ_{dp} is consistent with the Z_{dr} bias predicted for antenna errors of radar systems with LDR limit in the -30 dB to -35 dB range.

6. CONCLUSIONS

Simultaneous transmission of H and V polarization waves (termed SHV mode) is now a popular way to construct dual-polarization radar systems. The technique is based on the assumption of 1) zero-mean canting angle of the precipitation medium and 2) negligible antenna polarization errors. Zero-mean canting angle is a good approximation for rain but not for the ice phase of storms. SHV data from S-Pol during TiMERX showed Z_{dr} biases in the ice phase of storms are are likely due to a non-zero mean canting angle of the the ice particles. This corroborates well with Ryzhkov nd Zrnić (2007) similar findings.

Antenna errors were modeled and the Z_{dr} biases were examined when using SHV mode of operation. If a radar has an LDR measurement limit of $-30\,\text{dB}$ (determined from measurements in drizzle), then this errors corresponds to about $1°$ of either tilt or ellipticity angle polarization error. The bias in Z_{dr} is significant even for relatively low accumulation of ϕ_{dp} depending on the magnitude of the polarization errors and the relative phase of the H and V electric fields delivered to the antenna. To mitigate this problem, the H and V channel isolation need to be made low as possible.

Acknowledgment

Total ϕ_{dp}	Mean Z_{dr} (dB)	
	FHV	SHV
between 20 and 40 deg.	0.17	0.16
between 40 and 70 deg.	0.15	0.26
between 70 and 100 deg.	-0.07	0.02

Table 2: *A comparison of Z_{dr} values for HFV and SHV modes as a function of ϕ_{dp}. Reflectivities are limited to between 20 and 25 dBZ.*

References

Azzam, R.M.A. and N.M. Bashara, 1989: *Ellipsometry and polarized light*. North Holland, Amsterdam.

Bringi, V. and V. Chandrasekar, 2001: *Polarimetric Doppler Weather Radar*. Cambridge Univ. Press, Cambridge, UK.

Doviak, R., V. Bringi, A. Ryzhkov, A. Zahrai, and D. Zrnić, 2000: Polarimetric upgrades to operational WSR-88D radars. *J. Atmos. Oceanic Technol.*, **17**, 257–278.

Hubbert, J.C. and V.N. Bringi , 2003: Studies of the polarimetric covariance matrix: Part II: Modeling and polarization errors. *J. Atmos. Oceanic Technol.*.

McCormick, G.C., 1981: Polarization errors in a two-channel system. *Radio Sci.*, **16**, 67–75.

Ryzhkov, A. and D. Zrnić, 2007: Depolarization in icee crystals and its effect on radar polarimetric measurements. *J. Atmos. Oceanic Tech.*, **24**, 1256–1267.

Tapping, K.: 2001, Antenna calibration using the 10.7 cm solar flux. *Radar Polarimetry for geoscience applications*, P. Smith, ed., American Meteorological Society, http://cdserver.ametsoc.org/cd/ 010430_1/RADCAL_Links_2_Presentations.html.

Tragl, K., 1990: Polarimetric radar backscattering from reciprocal random targets. *IEEE Trans. Geosc. and Remote Sen.*, **8**, 856–864.
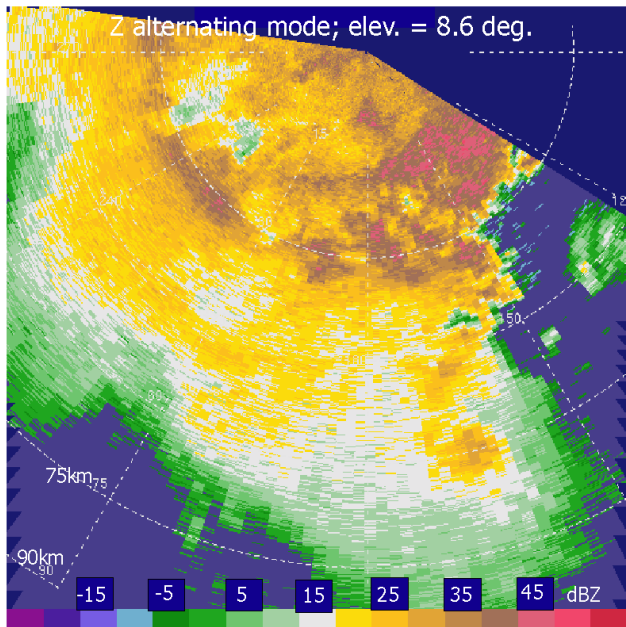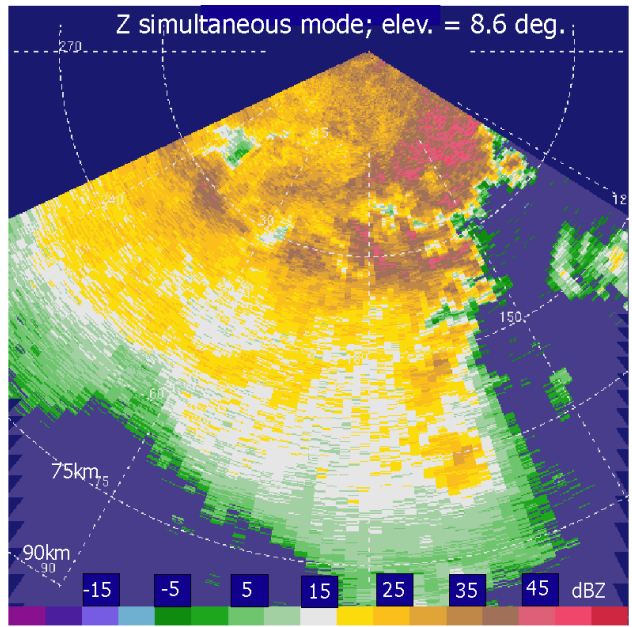
Figure 8: *FHVmode reflectivity for 8.6° elev.*
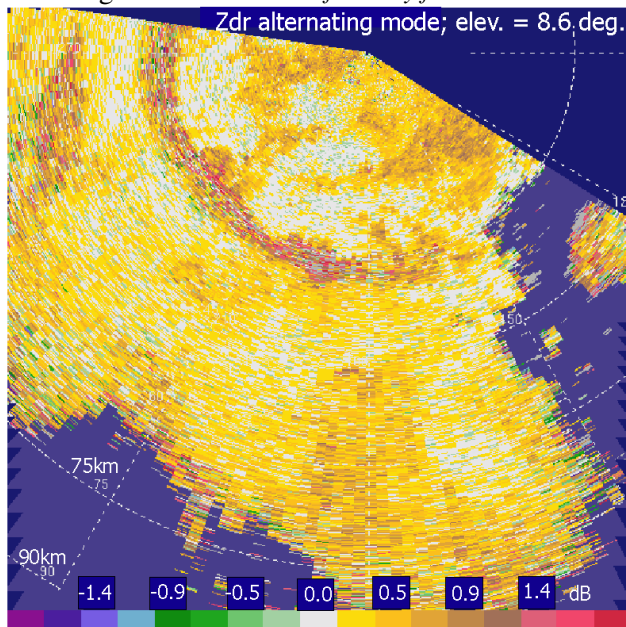

Figure 10: *SHVmode reflectivity for 8.6° elev.*

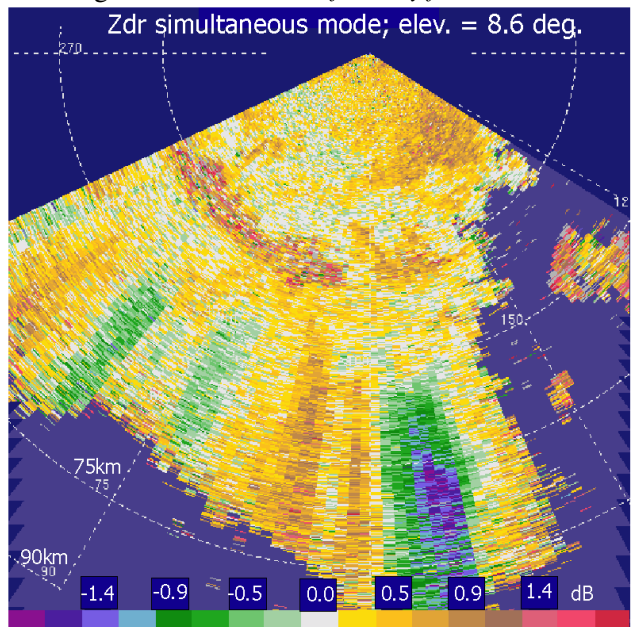Figure 9: *FHV mode Z_{dr} for 8.6° elev. corresponding to Fig. 8.*

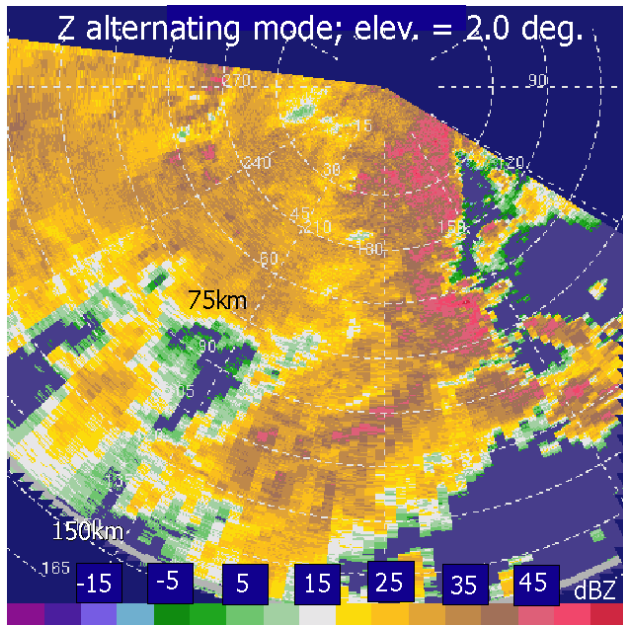Figure 11: *SHV mode Z_{dr} for 8.6° elev. corresponding to Fig. 10.*
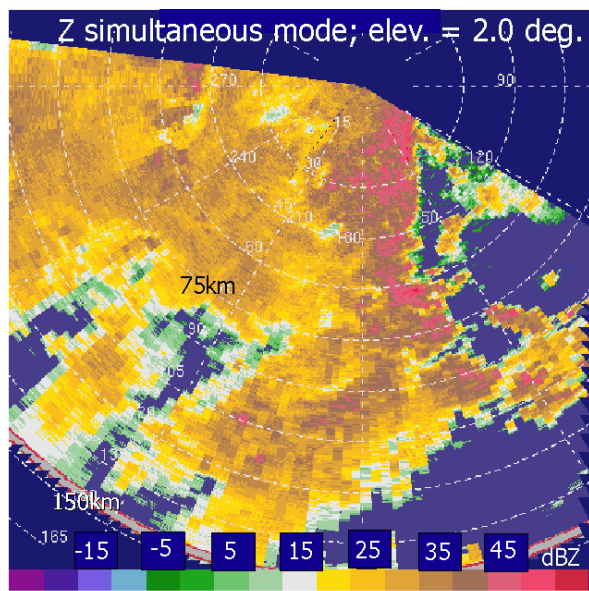
Figure 12: *FHVmode reflectivity for 2.0° elev.*

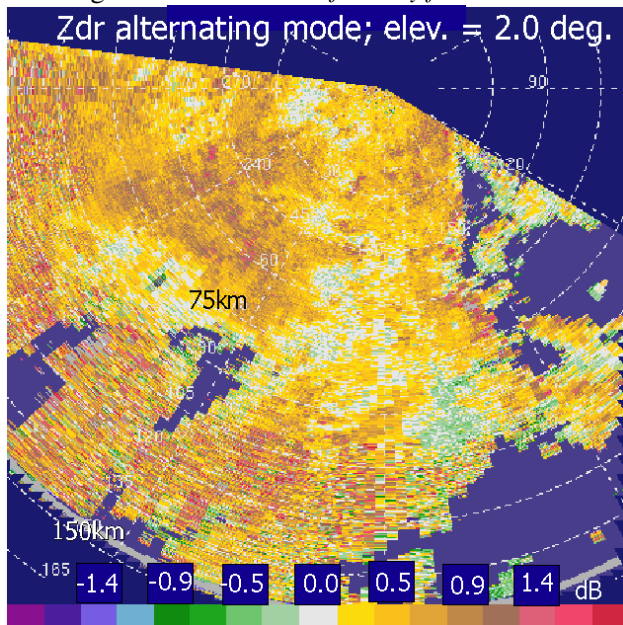Figure 14: *SHVmode reflectivity for 2.0° elev.*

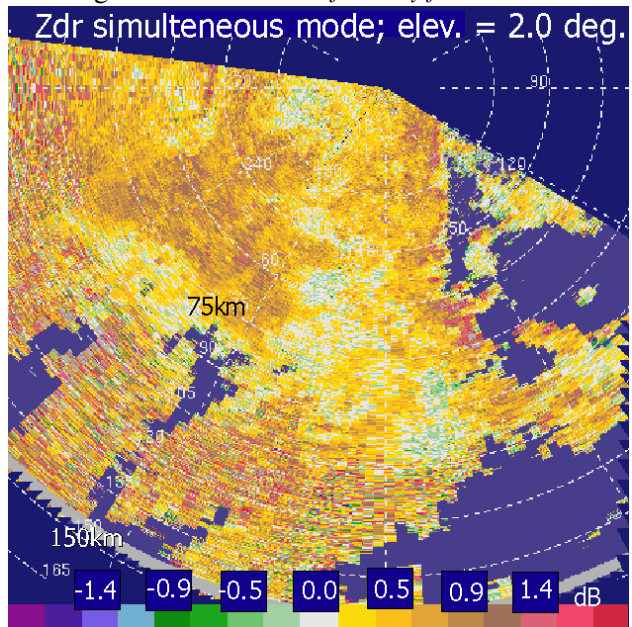Figure 13: *FHV mode Z_{dr} for 2.0° elev. corresponding to Fig. 12.*

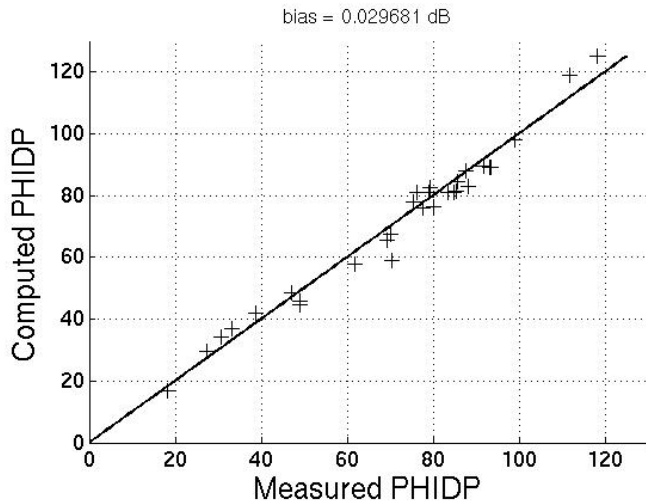Figure 15: *SHV mode Z_{dr} for 2.0° elev. corresponding to Fig. 14.*

Figure 16: *Scatter plot of calculated ϕ_{dp} (from Z and Z_{dr}) versus measured ϕ_{dp} from TiMREX FHV data. The Z bias is about 0.03 dBZ.*
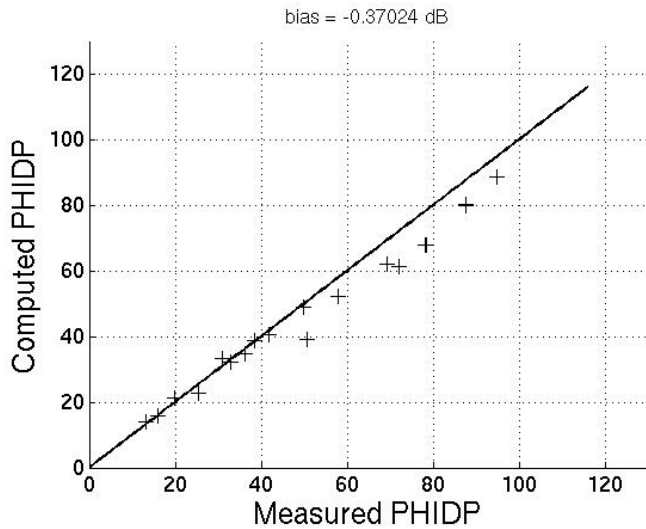

Figure 17: *Scatter plot of calculated ϕ_{dp} (from measured Z and Z_{dr}) versus measured ϕ_{dp} from TiMREX SHV data. The Z bias is about -0.37 dBZ but this is not the cause of the bias of the points for high ϕ_{dp}. It is bias of Z_{dr} for high ϕ_{dp} which is the cause.*

van de Hulst, H.C. , 1957: *Light scattering by small particles*. New York: Wiley.

Vivekanandan, J., G. Zhang, S. Ellis, D. Rajopadhyaya, and S. Avery, 2003: Radar reflectivity calibration using differential propagation phase measurement. *Radio Sci.*, **38**, 8049.

Vivekanandan, J.V., W.M. Adams and V.N. Bringi, 1991: Rigorous approach to polarimetric radar modeling of hydrometeor orientation distributions. *J. Appl. Meteorol.*, **30**, 1053–1063.

Wang, Y. and V. Chandrasekar, 2006: Polarizatioin isolation requirements for linear dual-polarization weather radar in simultaneous transmission mode of operation. *IEEE Trans. Geosc. and Remote Sen.*, **44**, 2019–2028.

Waterman, P.C., 1969: Scattering by dielectric particles. *Alta Frequeza,(Speciale)*, 348–352.